

National Radio Astronomy Observatory, Socorro, NM 87801

Very Large Array Program

VLA ELECTRONICS MEMORANDUM NO. 216

CLOSURE ERRORS IN THE VLA

D. S. Bagri

November 1990

SUMMARY This memorandum reviews different sources of closure errors in the VLA. Unequal bandpass responses and errors in the quadrature networks used in the samplers are the major contributors of such closure errors. For continuum observations, using 25 or 50 MHz bandwidths, about half of the closure errors are caused by amplitude and phase errors in the quadrature networks. Setting the delays accurately reduces the closure errors and improves their stability. Therefore it is suggested that the fixed delays be set to ≤ 1 ns accuracy. From test observations it is found that sources of closure errors are sufficiently stable over periods of several days to allow antenna gain calibration to about 0.1 – 0.2% accuracy.

1. INTRODUCTION

(a) What are closure errors? Closure errors are non-factorable errors in calculating complex gains for various antennas from the array calibration equations of the form (Cornwell 1985):

$$V_{mn} = G_m G_n^* G_{mn} R_{mn} + e_{mn} + N_{mn} \quad (1)$$

Here V_{mn} are the measured visibilities, R_{mn} are the estimates of the true visibilities, G_k is the complex gain of the k^{th} antenna, e_{mn} are the offset terms, N_{mn} are the system noise terms, and the subscripts m and n refer to antennas m and n. The accuracy of the estimated antenna gains, G_k , depends on the offset terms e_{mn} , and deviation from unity of the non-factorable terms G_{mn} . Closure errors are defined as deviations from unity of the non factorable terms G_{mn} ; i.e. closure error, α_{mn} , for the baseline formed by antennas m and n is given by:

$$\alpha_{mn} = G_{mn} - 1 \quad (2)$$

(b) Closure errors are multiplicative. With careful design of the hardware it is possible to minimize the offset terms. This has been achieved in the VLA by incorporating phase switching of the local oscillator signals at the antennas, using Walsh functions (Granlund, et al. 1978), and removing the phase switching from the signals after sampling. For calibration sources of moderate strength, stronger than a few Jy, noise terms N_{mn} are negligible and may be ignored. The closure errors α_{mn} for the observations of calibration sources from a few Jy to about 60 Jy at 6 cm (e.g. for 1600+335, OJ287, 2134+004 and 3C84 having flux density of about 2, 5, 10 and

60 Jy respectively) are independent of the source strength. This indicates that the offset terms e_{mn} are negligible, and can be ignored, and that the closure errors are essentially multiplicative. Note that the errors due to the present method of estimating the correlation coefficients, using square root of the product of self counts of the two signals for normalization, instead of proper application of the quantization correction is $\leq 0.1\%$ for correlation coefficients of upto 0.1 (Schwab 1985, Private communication), and therefore may be ignored for most practical purposes.

(b) Effects of closure errors. As pointed out by Clark (1981) the rms error in a map is proportional to $[(\sqrt{\langle w^2 \rangle} / \langle w \rangle) \sqrt{\alpha_{mn}^2}]$, where w is the weighting function and α_{mn} is the closure error for the baseline formed by antennas m and n . Thus, to obtain a high dynamic range, we need to minimize the rms closure error. Until about 1984, closure errors in the VLA were much higher than 1% (e.g. Walker 1984); the design goal for the VLA was to achieve closure errors $\leq 1\%$. Adjustments of the quadrature networks and the samplers have reduced both the amplitude and the phase closure errors to about 0.6 to 0.8% rms. It may be pointed out that for an eight hour synthesis with the VLA, assuming a limit of 100,000 for the dynamic range, images would be limited due to the closure errors rather than due to the system noise, for a large number of sources. Therefore, as pointed out by Perley (1985) and Walker (1984), it is important to devote some efforts to understand sources of closure errors and how they can be reduced or their affect can be minimized by "calibration".

2. SOURCES OF CLOSURE ERRORS

Sources of closure errors in the VLA have been discussed by Clark (1978), Thompson (1980), and Thompson and D'Addario (1982). These are described below:

(a) Non identical bandpass responses for various antennas. Closure errors due to variations in the frequency responses of different antennas have been discussed by Thompson (1980). He has worked out some representative examples of closure errors due to frequency response mismatches. The results are summarized below:

(i) Amplitude slopes. An amplitude slope of 3 dB between the band edges may give rise to a maximum of about 1% amplitude closure error.

(ii) Differences in the passband center frequency. Phase closure errors are zero and amplitude closure errors are approximately linear with maximum error of about 1% for a center frequency off-set of 3.2%.

(iii) Ripples in the bandpass. Phase closure errors are zero and amplitude closure errors of maximum about 1% for a peak to peak ripple of 2 dB over the bandpass.

(iv) Delay errors. Phase closure errors are $\leq 0.1\%$ and amplitude closure error have a dependence on the delay error (τ) which lies between linear and quadratic and a maximum closure error of about 1% occurs for $\Delta\tau = 0.05/\text{bandwidth}$. This corresponds to a delay error of 1 ns for the bandwidth of 50 MHz.

(v) Combination of the delay and passband errors. The phase closure errors are approximately proportional to the delay errors. For example a 2 dB ripple across the passband gives a maximum closure error of about 1% for a delay error of 1 ns using 50 MHz bandwidth. The amplitude closure error is the sum of the errors due to the delay errors and the passband ripples individually.

(vi) Anomalies at the edges of the passband. In the VLA bandpass characteristics for each signal is essentially determined by the back end filters at the baseband. These filters are generally low pass filters, designed to provide maximum variations of $\pm 1\%$ in the 3 dB bandwidth. VSWR over

80% of the 3 dB bandwidth be ≤ 1.5 . Mismatch of the filters over 90% of the bandwidth ≤ 0.2 dB in the amplitude and $\leq 5^\circ$ in the phase. Over the remaining 10% of the bandwidth amplitude mismatch ≤ 0.3 dB and phase mismatch $\leq 20^\circ$. This should cause $\leq 0.1\%$ phase closure errors and $\leq 0.5\%$ amplitude closure errors. Values of closure errors as a function of channel numbers in spectral line observing mode are shown in Table 1a. Large closure errors are caused at both ends of the baseband due to the bandpass errors. Also amplitude closure errors are larger than phase closure errors, which is consistent with the assumption that these errors are caused by the bandpass mismatches at the baseband.

(b) Delay errors. Most causes of closure errors discussed above give rise to predominantly amplitude closure errors. The phase closure errors arise essentially if the delays are incorrect. Approximately equal magnitude of the amplitude and the phase closure errors observed in the VLA continuum observations suggest that we need to set the delays more accurately. At present delay errors of upto 2 ns are allowed before updating the fixed delays. This is combined with other sources of delay errors; i.e (i) the delay stepping accuracy of ± 0.3 ns, (ii) the clock phase setting accuracy of $\approx 10^\circ$ and 1 dB giving rise to ≈ 0.5 ns delay error, and (iii) delay variations due to the path length changes in the waveguide transporting signals from the antenna vertex rooms to the central electronics room. In addition, affects of the timing errors in the samplers and threshold errors in the quantizers are equivalent to the delay errors (D’Addario, et al. 1984). When all these errors are combined, the overall maximum delay error may be close to 3 ns or even more.

Therefore, minimizing errors in the fixed delays may help reduce the closure errors. Test observations indicate that when the fixed delays are set carefully having ≤ 1 ns error, the closure errors are slightly lower and further they are more stable with time, and therefore can be calibrated. Also, when error in the fixed delay value for a particular antenna is large, the closure errors for baselines formed with that antenna are large. Thus we should make efforts to set fixed delays as accurately as possible. Thompson and D’Addario (1982) had recommended to set the delays to ≤ 1 ns accuracy.

(c) Errors in the quadrature networks. Most sources of closure errors described above require delay errors to explain the phase closure errors. The phase closure errors are proportional to the delay error divided by the bandwidth. Therefore, for the given delay errors, if the bandwidth is decreased, the closure errors should go down proportionately. However, both the amplitude and the phase closure errors increase when the bandwidth is decreased (Table 1b). Also, when the observations are made in the spectral line mode, both amplitude and phase closure errors are smaller (Table 1a), and further the phase closure errors are \leq half of the amplitude closure errors. This shows that errors in the quadrature networks contribute significantly to the closure errors in continuum observations. It should be noted that the spectral line observations are made without utilizing the quadrature property of the quadrature networks; i.e. both lag and lead signals from either the sine or the cosine sides of the quadrature networks from various antennas are cross correlated and Fourier transformed to generate complex correlation coefficients for each spectral channel.

The quadrature networks are all-pass 8 pole LC filters, and had achieved $\leq 1^\circ$ quadrature error over 1 to 50 MHz bandwidth on bench. In practice the quadrature is adjusted to $\approx 2^\circ$ phase error over 3 to 50 MHz range, and have larger errors below 3 MHz. Only phase quadrature is checked between the sine and the cosine sides of a given sampler unit, but amplitudes may differ

by as much as 0.5 to 1 dB over the 50 MHz bandwidth. Also, repeatability between different sampler units is not checked. These problems, along with (i) the poor coupling at the low frequency end in the transformers used in the samplers, (ii) different cable lengths between the D racks in the central electronics room and sampler inputs, and (iii) a VSWR of 1.5 for 80 MHz low pass filters used at the input of the screen room, may cause different amplitude and phase ripples and slopes for each baseband signal.

(d) Miscellaneous. Apart from the sources of closure errors discussed above, there are several other sources which may cause closure errors at some what lower levels. These are described below:

(i) Antenna polarization mismatch. Thompson (1984) has discussed the problem of closure errors due to polarization mismatch between various antennas. For small errors in antenna polarization parameters ϕ and θ (where ϕ = position angle of the polarization ellipse, and θ = arctan of the ratio of the two axes of the polarization ellipse), the Stoke's parameter I for the baseline formed by antennas m and n, for the circular polarization case, may be written as:

$$I = [1 - \frac{(\Delta\Phi_{mn}^2 + \Delta\Theta_{mn}^2)}{2} + i\Delta\Phi_{mn}]e^{i\Psi_{mn}} \quad (3)$$

where $\Delta\Phi_{mn} = \phi_m - \phi_n$, $\Delta\Theta_{mn} = \theta_m - \theta_n$, $\Psi_{mn} = \psi_m - \psi_n$, and ψ_k = argument of the complex gain for the k^{th} antenna.

Though passband ripples due to the feed and front end mismatches, and rotation of the beam as a source moves in the sky are antenna dependent, as the errors caused are non-linearly dependent on the phase difference between complex gains for the antennas, they contribute to the closure errors.

Model calculations for a six-antenna array using circularly polarised feeds, as in the VLA, indicate that an axial ratio of 1.12 for the polarization ellipse produces closure errors of amplitude 0.5% rms and 1% maximum (Thompson 1984). For the VLA feeds the axial ratio is less than 1.07. The mechanical setting error of the feed polarization axes on the sky should not be greater than about 1°. Thus the expected magnitude of the closure errors resulting from differences in the feed characteristics should be much less than 0.5%, if the source is near the center of the beam. Note also that it should be possible to calibrate the cross polarization terms by including them in the solution for the antenna gain, using all polarization products (or even only two parallel-hand terms), but this has yet not been tried in practice.

(ii) Finite image rejection in single sideband mixers (used for conversion of the IF signals to baseband in the T3 modules). The error in a correlator output, due to the finite image rejection ϵ_1 and ϵ_2 in the two baseband signals, at a baseband frequency ν may be expressed as $\epsilon_1\epsilon_2\exp(i2\pi\nu\tau)$, where τ is the difference between the compensating delays used. This results in a contribution to the output which depends on the image rejection and the delay difference, and therefore causes closure errors. Checking a few SSB mixer units gives typical values for image rejection of about 26-28 dB, and in some cases ≤ 24 dB, which may cause closure errors of $\approx 0.1\%$. It may cause large closure errors for smaller bandwidths, especially when the front end filter has much wider bandwidth, compared to overall system bandwidth. Also larger errors may be caused if the frequency setting of the Fluke synthesizer (final local oscillator used for converting the antenna signal to baseband) is not near the edge of the IF passband (i.e. there is substantial power due to the image sideband).

(iii) Sampler errors. There are several sources of errors in the samplers. These are described below:

(a) DC offset and phase switching. Though a small DC offset can cause a large error in the measured correlation coefficient, a relatively error free correction is obtained by phase switching (Granlund, et al. 1978). D'Addario, et al. (1984) have discussed the effect of the phase switching, and find the relative error $\leq 0.1\%$ for threshold levels within 10% of the optimum value. The effect of the phase changes during a phase switching cycle and errors caused due to the finite fringe phase step of 0.72° are considered negligible.

(b) Variations in the quantization thresholds. Effect due to variations of the quantization levels from the optimum value was first discussed by Thompson (1973). At present the measured cross correlation coefficient is normalized, in the VLA, using square-root of the product of self counts from each of the two samplers. Error in the measured correlation coefficient due to the normalization using product of the self counts, instead of proper quantization corrections, have been studied in detail by D'Addario, et al. 1984. Schwab (1985, Personal communication) has calculated that the resultant closure errors, due to the threshold level variations of upto 10% from the optimum value, are $\leq 0.1\%$ for correlation coefficients of ≤ 0.1 . A discussion of numerically attractive approximations for estimating true correlation coefficients, from the measured correlation coefficients and estimates of quantizer threshold settings, is given by Schwab (1978).

(c) Sampler timing errors. Effect of quantizer indecision, aperture time errors, quadrature timing errors, and sign and magnitude sampling time errors can all be considered to cause equivalent delay error (D'Addario et al. 1984). The contribution to the closure errors due to the practical values of these imperfections in the VLA should be $\leq 0.1\%$.

(iv) Injected noise calibration signal and ALC. D'Addario (1979) has studied the effect of injected noise calibration signal and ALC on gain errors. Effect of the injected noise and ALC will look like error in the antenna gain. This will have only a second order effect, and the resultant errors are $\leq 0.1\%$.

(v) Gain variations due to antenna tracking errors. It will have the effect on the antenna gain and can be bad for large sources. The antenna pointing errors may give rise to closure errors due to cross polarization, which may be important.

(vi) Short term atmospheric phase variations. The closure errors increased slightly (5 to 10%) during cloudy weather conditions, when the integration was increased from 10 to 30 sec for 6 cm observations in the A configuration. During this period typical (antenna gain) phase variations observed were about $10\text{-}20^\circ/\text{min}$. This is due to fall in coherence, and variations of the closure errors with the change in the arguments of the antenna gains. This indicates that short term atmospheric phase variations may be important for stability of the closure errors, especially at high frequency bands.

(vii) Cross-talk. The cross-talk between various adjacent antennas is a possible and likely source of closure errors in the D configuration at low elevation angles. Though we have not made any particular tests for this, the rms closure error does not increase noticeably when the physical shadowing is avoided.

Even though each of the above sources may cause only a small contribution to the closure errors; their combined effect may be important, especially when we want to achieve overall closure

errors of $\approx 0.1\%$ or try to calibrate the closure errors to this accuracy. Therefore efforts should be made to minimize each of these.

3. SOURCES OF CLOSURE ERRORS ARE DISTRIBUTED

It is possible to obtain two values of both the real and imaginary parts of a visibility measurement in continuum observations. Consider observing all the four cross products between the sine and cosine outputs of the quadrature networks of the two antennas m and n . The real part of the visibility can be obtained by either multiplying the cosine output from antenna m with the cosine output from the antenna n , or by multiplying the sine outputs from the two antennas. Similarly, two versions of the imaginary part of the visibility can be obtained. In normal operations only one value from each of the two pairs is retained, since the other value should give the same result if there were no errors in the quadrature networks or samplers. Consider observations in which both sets of visibility data are recorded. Taking difference of closure errors for the two versions of real as well as the two versions of imaginary parts of the visibility sheds light on whether the closure errors arise before the quadrature networks or in the quadrature networks and samplers. If the closure errors arise before the quadrature networks they would be completely correlated in the two measurements of the real, as well as two measurements of the imaginary parts of the visibility data. On the other hand the errors would be completely uncorrelated if they arise in the quadrature networks or samplers. Observations were made in which closure errors for both versions of each of the real and the imaginary parts, and their differences were recorded. The rms values of these measurements are given Table 2a. The correlations between closure errors of the two sets of the real visibility data and two sets of the imaginary visibility data represent the fraction of the closure errors arising before the quadrature networks. These are shown in Table 2b. The results indicate that only a part of the closure errors arise before the quadrature networks. These results, along with the comparison of the closure errors for the continuum and the spectral line observations (Tables 1a,b), are consistent with about half of the closure errors being contributed by the errors in the quadrature networks in the continuum observations. Another important contributor is dis-similar band edges as can be seen from the results in Tables 1a and 1b. The sources of remaining closure errors are distributed.

4. EFFECT OF PHASING THE ARRAY ON CLOSURE ERRORS

(a) Closure errors with phased array. 3C84 was observed at 6 cm in the A configuration in the continuum without phasing the array (standard mode) and with the phased array (VX mode), using bandwidths of 50, 12 and 3 MHz for approximately 5 min. each. All the observations were repeated immediately following the first set of observations as described above. The rms closure errors for these observations are given in Table 3a, and the rms of the differences of the closure errors (which show the stability of the closure errors) for the two sets of corresponding observations for each mode and bandwidth are given in Table 3b. Note that in the VLA only the A and D IFs are hardware phased. A study of the closure errors and their difference for the phased array continuum mode and their comparison with those in the standard continuum mode shows following interesting points:

(i) In the phased array continuum mode, compared to the standard continuum mode, the rms of closure errors for the real part of the visibility decrease and for the imaginary part of the visibility increase for the A and D IFs but essentially remain unaltered for the B and C IFs. (ii) On time scales of 1 hour and during good weather, values of both the real and imaginary parts of the closure errors, for all the four IFs, are stable to 0.1 to 0.15% (for 50 MHz bandwidth) in the phased array continuum observing mode. In comparison for standard continuum (without phasing the array) the stability of the closure errors is a factor of about 3 to 6 worse for all the 3 bandwidths (50, 12, and 3 MHz) used for the tests.

(iii) The stability of the phase closure errors is much better compared to the stability of the amplitude closure errors in the phased array mode for the A and D IFs, even though phasing the array reduces the rms amplitude closure errors and increases the rms phase closure errors. On the other hand the stability of both the amplitude and the phase closure errors is similar for the B and C IFs.

(iv) The stability of the phase closure errors for the B and C IFs is worse compared to that for the A and D IFs in the phased array mode. The stability of the amplitude closure errors is generally better for the B and C IFs compared to that for the A and D IFs.

2134+004 was observed in the A array at 6 cm using 25 MHz, 16 channel with hanning smoothing in the spectral line for about 5 min. each without phasing and with phasing the array. The observation were repeated in about half an hour, and again about 24 hours later. RMS of the closure errors for the above observations are given in Table 5. The rms of the differences of closure errors for observations half an hour apart on the two days, and 24 hours apart are given in Table 6. Following interesting points may be noticed from a study of the closure errors and their differences in Tables 4 to 6: (a) closure errors are much smaller for the psuedo continuum formed from the spectral line observations using central three quarter spectral channels (channel 0), compared to the standard continuum observations (Table 4), (b)for the channel 0 data phase closure errors are smaller compared to the amplitude closure errors by a factor of 2 (Table 4), (c) phasing the array reduces both amplitude and phase closure errors, and (d) stability of the closure errors for channel 0 for the phased array spectral line observations is $\leq 0.1\%$, and is better by a factor of 2-2.5 compared to the unphased array.

(b) Why phasing stabilizes closure errors? To understand the effect of phasing on the closure errors, consider the interferometer formed by antennas m and n, as shown in Fig.1. With reference to the notation given in Fig.1, the real and imaginary parts of the visibility for the baseline formed by antennas m and n may be written as:

$$\begin{aligned} Re[V_{mn}] &= \langle \cos(\theta_m + \Delta_{cm})\cos(\theta_n + \Delta_{cn}) \rangle \\ &= \cos\Theta_{mn}\cos(\Delta_{cm} - \Delta_{cn}) - \sin\Theta_{mn}\sin(\Delta_{cm} - \Delta_{cn}). \end{aligned}$$

This may be simplified as:

$$Re[V_{mn}] \simeq \left[1 - \frac{(\Delta_{cm} - \Delta_{cn})^2}{2}\right]\cos\Theta_{mn} - (\Delta_{cm} - \Delta_{cn})\sin\Theta_{mn} \quad (4)$$

For small values of Δ error terms, this can be further simplified to give:

$$Re[V_{mn}] \approx \cos\theta_{mn} - (\Delta_{cm} - \Delta_{cn})\sin\Theta_{mn} \quad (5)$$

Similarly we can write for imaginary part of the visibility as:

$$Im[V_{mn}] \approx \sin\Theta_{mn} - (\Delta_{cm} - \Delta_{sn})\cos\Theta_{mn} \quad (6)$$

From eqs. (5) and (6) we can see that the measured visibility are effected by difference of error terms multiplied by $\sin\Theta_{mn}$ for the real part of the visibility and $\cos\Theta_{mn}$ for the imaginary part of the visibility. Phasing the array forces $\Theta_{mn} = 0$ for the A and D IFs at the hardware multiplier point. Thus, the error contribution to the measured visibility is made stable with time for the A and D IFs, provided the Δ 's are not varying with time. Also, on short time scales, where almost all the phase variations are caused by atmosphere, phases of the B and C IFs are made stable; however their phases vary over time scales of several hours due to variations in the electronics (including waveguide etc.). This explains the measurements (Tables 4-6) of closure errors with and without phasing the array. When we consider both the amplitude and phase errors in the quadrature networks (see Fig. 2) the equations become more complicated but the basic point, that phasing the array stabilizes the contribution due to errors, remains valid.

(c) Stability of the sources of closure errors. From the results described and the analysis given above, it seems encouraging that the error terms can be either calibrated or estimated provided they are stable with time. Naturally the question arises about the extent and duration over which the imperfections causing the errors are stable, so that the errors can be corrected and/or calibrated. To examine this question, measurements of the closure errors on 3C84 (Tables 3a,b) and on 2134+004 (Tables 5 and 6) made at 6 cm in the A configuration may be used. These observations were made with separation in time from about half an hour to about 24 hours. Also during this period 1803+784 and OJ287 were observed to provide data on the closure errors every few hours. The rms closure errors and rms of the difference of closure errors for these observations are given in Tables 3,5, and 6. From the results it is clear that the sources of closure errors are stable giving rms closure errors $\approx 0.1\%$ over 24 hours, if the array is phased. The phased array observations of 1803+784 and OJ287 along with 2134+004 (Table 7) agree with this conclusion basically, though the stability of the closure errors is a bit poor. This could be due to the system noise and the structure in these sources at such a low flux density level.

To study the long term stability of the sources of the closure errors 3C84 was observed at 6 cm. Observations were made on 1986JUL04, 1986JUL07 and 1986JUL21 in continuum mode with and without phasing the array and using various bandwidths. Observations were also made in phased array spectral line mode (25 MHz, 16ch) on 1986JUL04 and 1986JUL07. The measured rms closure errors for the observations on the three days are given in Table 8. The rms of the differences of the closure errors for these three days are shown in Table 9. These results show that closure errors are stable to $\approx 0.1\%$ over several days.

(d) Problems of phasing the Array. The above observations indicate that the antenna gains can be calibrated to $\approx 0.1\%$ accuracy provided phasing of the array can be maintained. Apart from the fact that the hardware phasing is possible only for the A and D IFs, there are other problems of phasing the array. (i) Active phasing is possible only if there is a strong point sources present in the antenna beam. (ii) At the start of the phasing if argument of gain for one of the antenna is near 180° , it doesn't phase, and (iii) phases for some of the antennas, specially in the D IF, oscillate with peak to peak variations of $\approx 70^\circ$ and a period of 1 min. This behavior was observed during some of my test observations during 1985-86. The behavior occurred for several antennas every scan and antennas for which this occurred, changed from scan to scan. On one

occasion this behavior was also noted for one of the antennas in the A IF. The algorithm for phasing the array has since been modified and now the problems (ii) and (iii) of phasing are no longer important. (iv) There is a finite phase servo loop gain (0.25) and phase update takes place every 10 sec (integration period), and therefore during bad weather large phase variations may take place inspite of active phasing. Thus phasing accuracy is weather dependent and even at 6 cm during moderately cloudy weather stability of closure errors worsens by a factor of 2-3 as can be seen from observations of 3C84 (Table 10) and compare it with data on 2134+004 (Table 5). During this period phase stability of 20-30° peak were observed. Poor stability of closure errors at 2cm band, even in phased array mode, can be explained because of this. However the effect due to this can be minimised by decreasing the integration period.

5. CLOSURE ERRORS CAN BE CALIBRATED

From the review of different sources of closure errors and the discussion of various tests described above it is clear that sources of closure errors are distributed. About half of the closure errors arise in the quadrature networks, and the remaining sources of the closure errors are distributed over the entire system. Reducing the closure errors by a factor of 2 in the continuum may be possible by cutting off the spectrum below 1.5 MHz, but further substantial reduction in the closure errors by simple improvements to the hardware may be difficult.

Problems of calibrating the closure errors for high dynamic range mapping have been discussed in detail by Perley (1985). He reports achieving a dynamic range of 80,000 on 3C273 in the B configuration; highest previously achieved in a continuum observations with the VLA. To see whether phasing helps to stabilize closure errors, 3C84 was observed on 1986APR23 in the A configuration at 6 cm employing 50 MHz bandwidth in phased array (VA) mode. About 3 hours of data in continuum mode, for only the A and C IFs, spread over about 11 hours period, allowed to make an image of 3C84 having a dynamic range of 145,000 as shown in Fig. 3. The image was obtained using self cal and subtracting mean values of the closure errors for each baseline from the measured visibility data, as discussed by Perley for his map of 3C273 described above. This demonstrates that phasing helps stabilize closure errors. The closure errors can be calibrated to achieve larger dynamic range in the map. It should have been possible to get still higher dynamic range if (i) the data from the B and D IFs were also included in making the map; this was not done due to the problems of phasing the D IF described above, causing large errors in the phasing, and (ii) phasing errors for the A IF were not as large as 20° to 30°, due to the poor weather conditions.

6. CONCLUSIONS

(a) Major sources of closure errors are:

- (i) variations in bandpass responses,
- (ii) errors in the quadrature networks, and
- (iii) errors in setting compensating delays.

The contribution to closure errors due to bandpass variations are $\leq 0.2\%$, as seen in the observations using spectral line mode, specially if effects due to band edges are removed. More than half of the closure errors arise in the quadrature networks, a significant part of which are due to the errors below 1.5 MHz. Sources of remaining closure errors are widely distributed, but errors

contributed by these sources are not the limiting factor at this time in obtaining images of upto 200,000 dynamic range using the VLA.

Though improving the quadrature networks may be difficult, cutting off the spectrum below 1.5 MHz using high pass filters at the baseband may reduce the closure errors to roughly half of those present now. About half of the present (0.8% rms) closure errors are caused by several others sources before the quadrature networks. Reducing the imperfections of the quadrature networks (which is a difficult task) alone may not be enough to reduce the closure errors by a large factor. Trying to reduce the closure errors substantially by simple hardware improvements looks difficult.

(b) Fixed delays should be set as accurately as possible. A maximum error of 1 ns in setting the compensating delays, as suggested by Thompson and D'Addario (1982), seems a reasonable value. We need to understand the best way to determine the fixed delays, and whether the variations in the fixed delays are independent of the operating bands. For high dynamic range mapping it may be desirable to set the fixed delays to even 0.5 ns accuracy.

(c) Closure errors are considerably smaller (roughly a factor of 2 to 2.5) in spectral line mode for the Channel 0 (pseudo continuum formed using the central three quarter channels) even without band pass corrections. Rick Perley (private communication) obtained a dynamic range of 190,000 on 3C84 using pseudo continuum from 25 MHz, 16 channel spectral line observations at 6 cm (without either phasing the array or applying the bandpass calibration). However, observing in spectral line mode may not be a very useful way to achieve high dynamic range for many sources due to a decrease in signal to noise ratio because the maximum available bandwidth is reduced.

(d) Phasing helps stabilize closure errors both in the continuum and in the spectral line modes. Observations with the phased array in continuum mode have allowed to achieve a dynamic range of 145,000 on 3C84 in the A array using data from only the A and C IFs.

(e) Sources of closure errors seem sufficiently stable that it may be possible to estimate the extent of errors introduced by them in the measured visibility and then correct for them.

Briefly, there are many sources of closure errors, some at a few tenths of a percent level and several at ≤ 0.1 level. Setting fixed delays to 0.5 to 1 ns accuracy helps to reduce and stabilize the closure errors. Errors in the quadrature networks, specially those below 1.5 MHz, contribute a significant fraction of the closure errors. Cutting off the spectrum below 1.5 MHz, which causes this problem, may not be easy. It may be difficult to minimize contributions from all the sources to achieve closure errors $\leq 0.1\%$. On the other hand experiments show that the errors can be either calibrated using phased array observing mode or it may be possible to estimate the error terms in the visibility measurements and then apply corrections.

ACKNOWLEDGEMENTS

Most of this work was carried out in 1985-86 period. Several people participating in the VLA Test-Coordination meetings during this period have ably contributed in this study. Especially Peter Napier, Dick Sramek and Jack Campbell provided continuous encouragement; Ken Sowinski, Larry D'Addario, Frazer Owen, Craig Walker, Rick Perley, Barry Clark and Peter Napier

helped with several discussions. Ken Sowinski helped with software for some of the test observations and Chuck Broadwell helped in data reduction without which it would have been very difficult to make progress.

LIST OF TABLES AND FIGURES

Tables

- 1a. RMS closure errors as a function of channel number for (i) 25 MHz, 32 channel observations on 2134+004 without phasing the array, (ii) 25 MHz 16 channel with Hanning smoothing on 3C84 with phased array (VX), and its comparison with the 25 MHz continuum observation in phased array mode for the A IF.
- 1b. RMS closure errors as a function of observing bandwidth for (i) bandwidths of 25, 12, 6, 3, and 1.5 MHz on 3C84 at 6 cm, and (ii) backend filters of 12 and 6 MHz low pass and 8 MHz bandpass (JPL) filters on 3C286 at 6 cm.
- 2a. RMS closure errors and rms of the differences of the closure errors when all four cross products are observed. The cross products of A and B IFs normally discarded have been put in place of the normally observed product for C and D IFs respectively.
- 2b. Correlation between the closure errors obtained from the two sets of both the real and imaginary visibility measurements.
- 3a. RMS closure errors for the standard and phased array observing modes for continuum 50, 12 and 3 MHz bandwidths.
- 3b. RMS of the difference of closure errors for the two sets of observations in Table 3a, separated by about 1 hour.
4. Comparison of RMS closure errors for continuum and the Channel 0 (pseudo continuum formed by combining the central three quarter channels of a spectral line observation).
5. RMS of closure errors and the differences of closure errors for continuum observations made about 0.5 hour apart and 24 hours later.
6. Same as Table 5 above for the Channel 0 data of 25 MHz, 16 channel observations with Hanning smoothing.
7. RMS closure errors and rms of the differences of closure errors for the phased array observations on 2134+004, 1803+784 and OJ287 at 6 cm in the continuum with 50 MHz bandwidth.
8. RMS closure errors for the observations of 3C84 at 6 cm using different bandwidths, and with and without phasing the array on 1986JUL04, 1986JUL07 and 1986JUL21.
9. RMS of the differences of the closure errors measured for the three days in Table 8. This gives stability of the closure errors over the period of 17 days over which these measurements were made.
10. Closure errors and difference of the closure errors on 3C84 for the observations during cloudy weather conditions.

Figures

1. Block diagram to explain how phasing stabilizes closure errors
2. Same as Fig. 1 with both amplitude and phase errors.

3. Map of 3C84 with the phased array in the continuum mode. The map was made using data for only the A and C IFs, and the array was in the A configuration.

REFERENCES.

- Clark, B. G. 1978, VLA Electronics Memo. No. 171, NRAO, Socorro, NM.
- Clark, B. G. 1981, VLA Scientific Memo. No. 137, NRAO, Socorro, NM.
- Cornwell, T. 1985, in *Synthesis Imaging, Workshop held Aug. 5-9, 1985, Socorro, NM.*, eds. R. A. Perley, F. R. Schwab and A. H. Bridle, p. 137.
- D'Addario, L. R. 1979, VLA Electronics Memo. No. 186, NRAO, Socorro, NM.
- D'Addario, L. R., et al. 1984, *Radio Science*, 19, 931.
- Granlund, J. 1978, *IEEE Trans. Electromagn. Compat.*, *EMC-20(3)*, 451.
- Perley, R. 1985, in *Synthesis Imaging, Workshop held Aug. 5-9, 1985, Socorro, NM.*, eds. R. A. Perley, F. R. Schwab and A. H. Bridle, p. 161.
- Schwab, F. 1978, VLA Computer Memo. No. 150, NRAO, Socorro, NM.
- Thompson, A. R. 1973, VLA Electronics Memo. No. 112, NRAO, Socorro, NM.
- Thompson, A. R. 1980, VLA Electronics Memo. No. 192, NRAO, Socorro, NM.
- Thompson, A. R. 1984, VLB Array Memo. No. 346, NRAO, Socorro, NM.
- Thompson, A. R. and D'Addario, L. R. 1982, *Radio Science*, 17, 357.
- Walker, R. C. 1984, VLA Scientific Memo. No. 152, NRAO, Socorro, NM.

TABLE 1a: RMS closure errors as a function of channel number for:

(i) 25 MHz 32 channel observations on 2134+004 at 6 cm

CHANNEL NUMBER	CLOSURE ERRORS (%)	
	Re	Im
0	0.36	0.14
(SUM CH 4-28)	4.86	5.04
1	2.77	2.96
2	0.58	0.52
15	0.35	0.20
SUM(14 TO 18)	0.42	0.18
SUM(12 TO 30)	0.56	0.45
28	0.55	0.45
29	1.63	1.57
31	7.18	7.77

(ii) 25 MHz 16 channel with Hanning smoothing on 3C84 with phased array (VX), and its comparison with the 25 MHz continuum observations the with phased array

CHANNEL NUMBER	CLOSURE ERRORS (%)		DIFF. OF CLOSURE ERRORS (ODD CH. - EVEN CH.) %	
	Re	Im	Re	Im
1	0.3219	0.1052		
2	0.3167	0.0876	0.1039	0.0842
3	0.3139	0.0927		
4	0.3186	0.0878	0.0605	0.065
5	0.3194	0.0872		
6	0.3225	0.0850	0.0616	0.058
7	0.3189	0.0875		
8	0.319	0.0855	0.054	0.0599
9	0.3242	0.086		
10	0.3179	0.0893	0.0682	0.0568
11	0.3251	0.0995		
12	0.3232	0.0973	0.0644	0.0601
13	0.3212	0.1014		
14	0.3194	0.1049	0.0676	0.0629
15	0.3921	0.1254		
1 TO 15	0.3518	0.1289		
25MHz CONTINUUM (IF A)				
	0.370	0.636		

TABLE 1b RMS closure errors as a function of bandwidth for continuum observations

(i) with 25, 12, 6, 3 and 1.5 MHz bandwidth back end filters on 3C84 at 6 cm

BANDWIDTH MHz	TIME (IAT)		CLOSURE ERRORS (%) FOR IF							
	FROM	TO	A		B		C		D	
			Re	Im	Re	Im	Re	Im	Re	Im

86JUL04										
STANDARD CONTINUUM										
25	13:52:30	14:01:50	0.615	0.560	0.673	0.583	0.758	0.818	0.838	0.932
12	12:28:50	12:32:00	0.978	0.894	1.001	0.922	0.920	1.086	0.923	1.323
6	12:32:30	12:42:00	1.724	1.207	0.876	1.279	1.739	1.435	0.888	1.508
3	12:42:30	12:52:20	2.482	3.175	2.134	2.98	2.308	3.817	1.959	2.888
1.5	12:52:50	13:05:30	5.471	6.583	4.508	6.613	6.316	7.801	4.314	6.565
PHASED ARRAY CONTINUUM										
25	14:02:20	14:11:50	0.386	0.653	0.63	0.596	0.745	0.804	0.509	1.104
12	13:07:50	13:16:50	0.344	1.064	1.131	2.29	1.051	1.102	0.43	1.49
6	13:17:20	13:26:50	0.561	1.904	2.159	4.082	1.443	1.661	0.473	2.071
3	**		0.514	3.819	3.025	3.502	2.226	3.572	0.376	3.37
1.5	13:37:40	13:52:00	1.849	7.891	4.142	6.178	6.287	7.081	0.776	6.921
** 3 MHz DATA ON 86JUL04 HAD PROBLEM, THIS DATA IS FROM 87JUL21										

(ii) with 12 MHz, 6 MHz lowpass and 8 MHz bandpass (JPL 18.75/8 MHz) backend filters on 3C286 at 6 cm

SOURCE NAME:QUA	OBSERV. MODE	BW MHz	TIME (IAT)		% FOR IF							
			FROM	TO	A		B		C		D	
					Re	Im	Re	Im	Re	Im	Re	Im

3C286:1	STAND CONT	12(LPF)			1.025	0.938	1.034	0.913	1.127	1.059	1.11	1.14
3C286:2	STAND CONT	6(LPF)			1.279	1.649	1.302	1.564	1.502	1.744	1.366	1.745
3C286:3	STAND CONT	8(BPF)			0.672	0.827	0.673	0.72	0.681	0.675	0.674	0.81
3C286:11	STAND CONT	12(LPF)			0.725	0.841	0.772	0.817	0.883	0.966	0.862	1.006
3C286:12	STAND CONT	6(LPF)			1.194	1.572	1.254	1.464	1.414	1.669	1.273	1.651
3C286:13	STAND CONT	8(BPF)			0.667	0.829	0.0.680	0.686	0.688	0.661	0.667	0.799
DIFFERENCES FOR QUALIFIERS												
1-11	STAND CONT	12(LPF)			0.557	0.359	0.638	0.45	0.561	0.394	0.574	0.426
2-12	STAND CONT	6(LPF)			0.416	0.421	0.581	0.589	0.489	0.476	0.456	0.388
3-13	STAND CONT	8(BPF)			0.268	0.245	0.278	0.288	0.279	0.265	0.275	0.277

TABLE 2a

IF	% RMS CLOSURE ERRORS					
	REAL		IMAGINARY		ss-cc	sc+cs
	sin*sin (ss)	cos*cos (cc)	sin*cos (sc)	cos*sin (cs)		
A	0.823	0.842	0.778	0.693	0.832	1.06
B	0.909	0.992	0.727	0.763	0.643	0.784

TABLE 2b

IF	REAL	IMAGINARY
A	0.5	0.035
B	0.77	0.446

Table 3a

SOURCE NAME:QUA	OBSERV. MODE	BW MHz	TIME (IAT)		% FOR IF							
			FROM	TO	A Re	Im	B Re	Im	C Re	Im	D Re	Im
86MAR14					RMS CLOSURE ERRORS							
3C84:1	STANDARD	50	2:49:50	2:53:10	1.162	0.831	0.657	0.562	0.896	0.836	0.844	0.731
3C84:2	STANDARD	12	2:53:40	2:56:10	0.959	1.024	0.782	0.74	0.847	1.047	0.895	1.003
3C84:3	STANDARD	3	2:56:40	3:00:10	2.68	3.802	2.562	3.026	2.597	3.189	2.132	2.553
3C84:5	PHASED (VX)	50	3:03:40	3:06:15	0.636	0.961	0.656	0.563	0.887	0.811	0.715	0.619
3C84:7	PHASED (VX)	12	3:09:40	3:12:10	0.505	1.225	0.748	0.788	0.830	1.06	0.516	1.178
3C84:9	PHASED (VX)	3	3:15:40	3:18:10	1.436	3.765	2.448	3.071	2.429	3.17	1.102	3.121
3C84:21	STANDARD	50	4:06:20	4:10:00	1.129	0.769	0.676	0.582	0.895	0.859	0.807	0.716
3C84:22	STANDARD	12	4:10:30	4:13:00	0.90	1.073	0.765	0.769	0.865	1.022	0.823	1.021
3C84:23	STANDARD	3	4:13:30	4:17:00	2.507	3.563	2.48	3.042	2.573	3.143	1.977	2.676
3C84:25	PHASED (VX)	50	4:20:30	4:23:00	0.658	0.98	0.649	0.558	0.864	0.821	0.71	0.712
3C84:27	PHASED (VX)	12	4:26:30	4:29:00	0.49	1.236	0.75	0.796	0.814	1.072	0.486	1.196
3C84:29	PHASED (VX)	3	4:32:30	4:34:50	0.869	3.855	0.25	3.021	3.137	5.497	0.70	3.121

TABLE 3b

SOURCE NAME:QUA	OBSERV. MODE	BW MHz	TIME (IAT)		% FOR IF							
			FROM	TO	A Re	Im	B Re	Im	C Re	Im	D Re	Im
DIFFERENCES FOR QUALIFIERS					RMS OF DIFFERENCE OF CLOSURE ERRORS							
1-21	STANDARD	50			0.522	0.529	0.336	0.352	0.519	0.489	0.568	0.577
2-22	STANDARD	12			1.037	0.877	0.765	0.759	0.999	1.044	0.934	1.026
3-23	STANDARD	3			3.187	3.418	2.995	2.99	3.369	2.835	2.464	2.571
5-25	PHASED (VX)	50			0.133	0.095	0.107	0.112	0.168	0.169	0.148	0.101
7-27	PHASED (VX)	12			0.343	0.146	0.223	0.231	0.291	0.316	0.327	0.123
9-29	PHASED (VX)	3			1.283	0.523	1.117	1.23	2.249	4.58	0.958	0.38

TABLE 4

SOURCE NAME:QUA	OBSERV. MODE	BW MHz	TIME (IAT)		% RMS CLOSURE ERRORS FOR IF								
			FROM	TO	A Re	Im	B Re	Im	C Re	Im	D Re	Im	
			86APR08										
1803+784	STAND CONT	50	13:10:30	13:29:50	0.744	0.637	0.604	0.524	0.625	0.524	0.695	0.589	
2134+004	SPEC (1A)	25MHz 16CH	14:21:50	14:31:10	0.392	0.194							

TABLE 5
CONTINUUM OBSERVATIONS

SOURCE NAME:QUA	OBSERV. MODE	BW MHz	DATE	TIME (IAT)		% RMS CLOSURE ERRORS							
				FROM	TO	A Re	Im	B Re	Im	C Re	Im	D Re	Im
2134+004:8C1	PHASED (VA)	25	86APR08	14:25:30	14:34:40	0.373	0.852	2.06*	0.563	0.636	0.745	2.09*	0.944
2134+004:8C2	PHASED (VA)	25	86APR08	14:55:30	15:04:40	0.377	0.858	3.56*	0.546	0.642	0.76	3.63*	0.9
2134+004:9C1	PHASED (VA)	25	86APR09	14:31:50	14:40:40	0.393	0.856	0.586	0.578	0.662	0.747	0.409	0.96
2134+004:9C1	PHASED (VA)	25	86APR09	15:01:40	15:10:40	0.405	0.85	0.569	0.559	0.656	0.742	0.423	0.959
1803+784:CAL8	STANDARD	50	86APR08	13:10:30	13:29:50	0.744	0.637	0.604	0.547	0.625	0.524	0.695	0.589
1803+784:CAL9	STANDARD	50	86APR09	13:17:00	13:35:00	0.737	0.682	0.606	0.564	0.655	0.602	0.712	0.657
DIFFERENCES FOR QUALIFIERS				DURATION APART		%RMS OF DIFFERENCES OF CLOSURE ERRORS							
8C1-8C2	PHASED (VA)	25		ABOUT 30 min		0.133	0'09	4.11*	0.203	0.198	0.197	4.15*	0.241
9C1-9C2	PHASED (VA)	25		ABOUT 30 min		0.167	0.105	0.17	0.168	0.226	0.213	0.111	0.149
8C1-9C1	PHASED (VA)	25		ABOUT 24 Hrs.		0.128	0.15	2.18*	0.309	0.41	0.445	2.18*	0.221
8C2-9C2	PHASED (VA)	25		ABOUT 24 Hrs.		0.162	0.163	3.59*	0.329	0.438	0.446	0.336	0.239
CAL8-CAL9	STANDARD	50		ABOUT 24 Hrs.		0.336	0.339	0.363	0.339	0.467	0.498	0.389	0.387

* ==> BAD DATA

TABLE 6
SPECTRAL LINE, SINGLE IF (1A)

SOURCE NAME:QUA	OBSERV. MODE	BW MHZ	DATE	TIME (IAT)		IF			
				FROM	TO	A Re	Im		
%RMS CLOSURE ERRORS									
2134+004:8L1	STANDARD	25	86APR08	14:21:50	14:31:10	0.392	0.194		
2134+004:8L2	PHASED (VX)	25	86APR08	14:36:10	14:44:10	0.350	0.136		
2134+004:8L3	STANDARD	25	86APR08	14:45:10	14:54:40	0.401	0.224		
2134+004:8L4	PHASED (VX)	25	86APR08	15:07:20	15:14:20	0.351	0.136		
2134+004:9L1	STANDARD	25	86APR09	14:26:30	14:30:50	0.368	0.173		
2134+004:9L2	PHASED (VX)	25	86APR09	14:42:10	14:50:40	0.357	0.147		
2134+004:9L3	STANDARD	25	86APR09	14:51:10	15:00:40	0.60*	0.856*		
2134+004:9L4	PHASED (VX)	25	86APR09	15:14:50	15:20:40	0.361	0.154		
DIFFERENCES FOR QUALIFIERS				DURATION APART		%RMS OF DIFFERENCES OF CLOSURE ERRORS			
8L1-8L3	STANDARD	25		ABOUT 0.5 Hr.		0.256	0.245		
8L2-8L4	PHASED (VX)	25		ABOUT 0.5 Hr.		0.091	0.097		
9L1-9L3	STANDARD	25		ABOUT 0.5 Hr.		0.48*	0.86*		
9L2-9L4	PHASED (VX)	25		ABOUT 0.5 Hr.		0.113	0.099		
8L1-9L1	STANDARD	25		ABOUT 24 Hrs.		0.217	0.191		
8L2-9L2	PHASED (VX)	25		ABOUT 24 Hrs.		0.093	0.094		
8L3-9L3	STANDARD	25		ABOUT 24 Hrs.		0.49*	0.87*		
8L4-9L4	PHASED (VX)	25		ABOUT 24 Hrs.		0.119	0.11		

* ==> BAD DATA

TABLE 7
CONTINUUM OBSERVATIONS

SOURCE NAME:QUA	OBSERV. MODE	BW MHZ	DATE	TIME (IAT)		IF		B		C		D	
				FROM	TO	A Re	Im	Re	Im	Re	Im	Re	Im
% RMS CLOSURE ERRORS													
OJ287:1	PHASED (VA)	50	86APR09	04:38:00	04:47:50	0.60	0.792	0.570	0.602	0.599	0.566	0.610	0.696
OJ287:2	PHASED (VX)	50	86APR09	04:48:20	04:52:40	0.636	0.803	0.580	0.591	0.596	0.585	0.628	0.713
1803+784:1	PHASED (VA)	50	86APR09	09:58:30	10:05:50	0.640	0.815	0.644	0.624	0.639	0.583	0.625	0.711
1803+784:2	PHASED (VX)	50	86APR09	10:06:30	10:11:30	0.651	0.867	0.623	0.61	0.664	0.606	0.685	0.716
2134+004:1	PHASED (VA)	50	86APR09	15:21:00	15:27:00	0.639	0.752	0.569	0.551	0.605	0.539	0.590	0.691
2134+004:2	PHASED (VX)	50	86APR09	15:31:00	15:36:00	0.635	0.755			0.619	0.564		
1803+784:CAL	PHASED (VA)	50	86APR09	13:17:00	13:36:00	0.737	0.682	0.606	0.564	0.655	0.602	0.712	0.657
DIFFERENCES FOR				DURATION APART		% RMS OF DIFFERENCES OF CLOSURE ERRORS							
OJ287-1803	PHASED (VA)	50		ABOUT 5.5 Hrs.		0.306	0.258	0.438	0.464	0.372	0.371	0.354	0.329
OJ287-2134	PHASED (VA)	50		ABOUT 11 Hrs.		0.207	0.189	0.303	0.331	0.338	0.321	0.216	0.23
1803-2134	PHASED (VA)	50		ABOUT 5.5 Hrs.		0.299	0.257	0.373	0.389	0.398	0.347	0.282	0.284
OJ287-1803	PHASED (VX)	50		ABOUT 5.5 Hrs.		0.357	0.361	0.419	0.419	0.385	0.405	0.298	298
OJ287-2134	PHASED (VX)	50		ABOUT 11 Hrs.		0.259	0.247			0.369	0.356		
1803-2134	PHASED (VX)	50		ABOUT 5.5 Hrs.		0.325	0.32			0.41	0.341		

TABLE 8
CONTINUUM (CONT)/ SPECTRAL LINE (SPEC) OBSERVATIONS

SOURCE NAME:QUA	OBSERV. MODE	BW MHZ	DATE	TIME (IAT)		IF		B		C		D	
				FROM	TO	A Re	Im	Re	Im	Re	Im	Re	Im
						% RMS CLOSURE ERRORS							
3C84:1	STAND. CONT	25	86JUL04	13:52:30	14:01:50	0.615	0.56	0.673	0.583	0.758	0.818	0.836	0.932
3C84:2	PHASED CONT	25	86JUL04	14:02:20	14:11:50	0.386	0.653	0.63	0.596	0.745	0.804	0.509	1.104
3C84:3	PHASED SPEC	25,CH0	86JUL04			0.344	0.101						
3C84:11*	STAND. CONT	12	86JUL04	12:28:50	12:32:00	0.978	0.894	1.001	0.923	0.920	1.086	0.923	1.323
3C84:12*	STAND. CONT	6	86JUL04	12:32:30	12:42:00	1.724	1.207	0.876	1.279	1.739	1.435	0.888	1.508
3C84:13*	STAND. CONT	1.5	86JUL04	12:52:50	13:05:30	5.471	6.583	4.508	6.613	6.316	7.801	4.314	6.565
3C84:21*	PHASED CONT	12	86JUL04	13:07:50	13:16:50	0.344	1.064	1.131	2.29	1.051	1.102	0.43	1.49
3C84:22*	PHASED CONT	6	86JUL04	13:17:20	13:26:50	0.561	1.904	2.159	4.082	1.443	1.661	0.473	2.071
3C84:23*	PHASED CONT	1.5	86JUL04	13:37:40	13:52:00	1.849	7.889	14.142	6.178	6.287	7.081	0.776	6.921
3C84:1	STAND. CONT	25	86JUL07	12:11:00	12:20:10	0.625	0.581	0.616	0.569	0.664	0.825	0.874	0.906
3C84:2	PHASED CONT	25	86JUL07	12:20:40	12:30:10	0.382	0.641	0.646	0.566	0.808	0.761	0.520	1.113
3C84:3	PHASED SPEC	25,CH0	86JUL07			0.342	0.119						
3C84:11*	STAND. CONT	12	86JUL07	10:47:00	10:50:30	0.712	1.009	0.844	0.997	0.968	1.193	0.918	1.235
3C84:12*	STAND. CONT	6	86JUL07	10:51:10	11:00:30	2.571	2.109	1.859	1.744	2.424	2.133	1.383	1.688
3C84:13*	STAND. CONT	1.5	86JUL07	11:14:20	11:25:40	6.36	6.328	6.457	8.597	6.988	8.708	5.372	6.426
3C84:21*	PHASED CONT	12	86JUL07	11:26:10	11:35:20	0.348	1.075	0.794	1.062	0.832	1.306	0.429	1.533
3C84:22*	PHASED CONT	6	86JUL07	11:35:50	11:45:20	0.356	1.968	1.495	2.106	1.378	2.055	0.406	2.06
3C84:23*	PHASED CONT	1.5	86JUL07	11:56:10	12:10:30	1.501	7.719	4.13	6.896	4.989	8.021	0.939	6.921
3C84:1	STAND. CONT	25	86JUL21										
3C84:2	PHASED CONT	25	86JUL21	11:27:00	11:35:10	0.370	0.636	0.632	0.551	0.817	0.844	0.461	1.022
3C84:3	PHASED SPEC	25,CH0	86JUL21										
3C84:11*	STAND. CONT	12	86JUL21	08:51:30	09:00:40	0.595	0.608	0.637	0.811	0.641	0.893	0.647	0.857
3C84:12*	STAND. CONT	6	86JUL21	09:01:10	09:15:50	0.687	1.16	0.818	1.412	0.907	1.376	0.823	1.336
3C84:13*	STAND. CONT	1.5	86JUL21	09:31:00	09:45:50	2.639	4.744	3.245	5.549	2.995	5.73	1.819	4.224
3C84:21*	PHASED CONT	12	86JUL21	09:46:20	10:00:30	0.401	1.012	0.863	1.053	0.721	1.082	0.446	1.371
3C84:22*	PHASED CONT	6	86JUL21	10:01:00	10:15:40	0.621	1.965	1.535	1.762	1.662	1.79	0.513	1.987
3C84:23*	PHASED CONT	1.5	86JUL21	10:30:50	10:45:50	1.637	7.803	6.344	7.215	2.447	5.453	1.445	6.458

* = 13 NON P-BAND ANTENNAS (in 1986) USED FOR THESE TESTS
ARRAY CONFIGURATION WAS A/B ON 86JUL04 AND 86JUL07, AND B ON 86JUL21; ANTENNAS #1,16,26 MOVED DURING A/B TO B

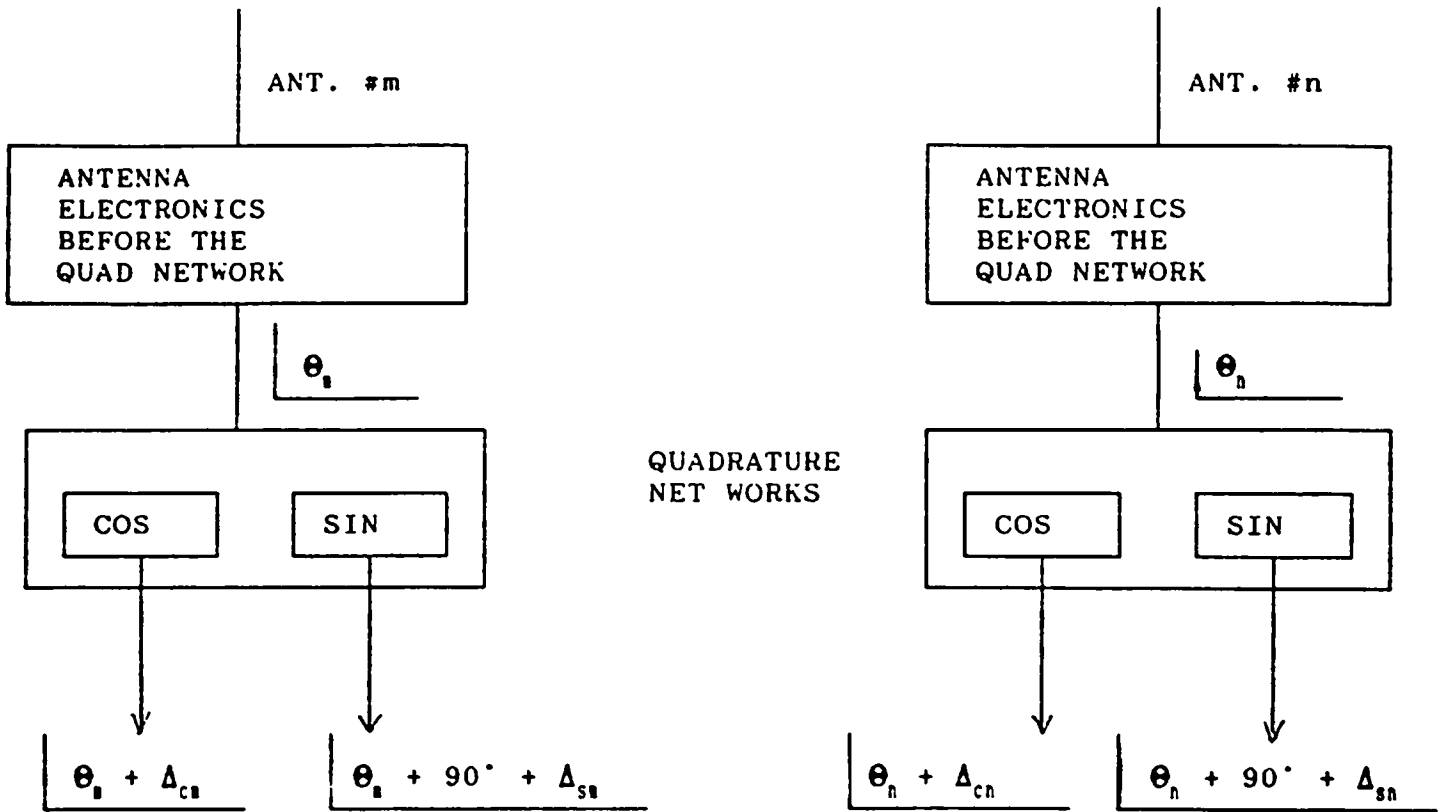
TABLE 9

DIFFERENCES	OBSER	MODE	BW(MHz)	DURATION	APART (*)	% RMS OF DIFFERENCES OF CLOSURE ERRORS								
	PHASED	SPEC	25, CH0	3	DAYS	0.075	0.083							
	PHASED	CONT	25	3	DAYS	0.097	0.147	0.540	0.551	0.784	0.864	0.104	0.10	
	PHASED	CONT	12	3	DAYS	0.132	0.131	1.186	2.224	1.274	1.263	0.257	0.14	
	PHASED	CONT	6	3	DAYS	0.463	0.349	2.451	4.122	1.926	2.083	0.295	0.43	
	PHASED	CONT	1.5	3	DAYS	1.124	0.95	5.533	6.072	7.91	7.72	0.421	0.15	
	PHASED	SPEC	25, CH0	14	DAYS*									
	PHASED	CONT	25	14	DAYS*	0.182	0.152	0.661	0.661	0.938	0.844	0.318	0.42	
	PHASED	CONT	12	14	DAYS*	0.219	0.256	1.064	1.231	1.101	1.245	0.327	0.49	
	PHASED	CONT	6	14	DAYS*	0.474	0.293	1.86	2.237	2.356	2.087	0.429	0.55	
	PHASED	CONT	1.5	14	DAYS*	1.122	1.279	7.458	8.127	5.908	5.805	2.05	0.77	
	PHASED	SPEC	25, CH0	17	DAYS*									
	PHASED	CONT	25	17	DAYS*	0.193	0.157	0.685	0.615	0.892	0.839	0.311	0.36	
	PHASED	CONT	12	17	DAYS*	0.258	0.26	1.331	2.385	1.186	1.317	0.47	0.46	
	PHASED	CONT	6	17	DAYS*	0.506	0.382	2.645	4.157	2.158	2.221	0.444	0.53	
	PHASED	CONT	1.5	17	DAYS*	0.779	0.732	7.363	7.444	6.411	6.138	1.923	0.75	

* = ARRAY CONFIGURATION CHANGED FROM A/B TO B BETWEEN TWO SETS OF DATA DIFFERENCED

TABLE 10
CONTINUUM OBSERVATIONS AT 6cm

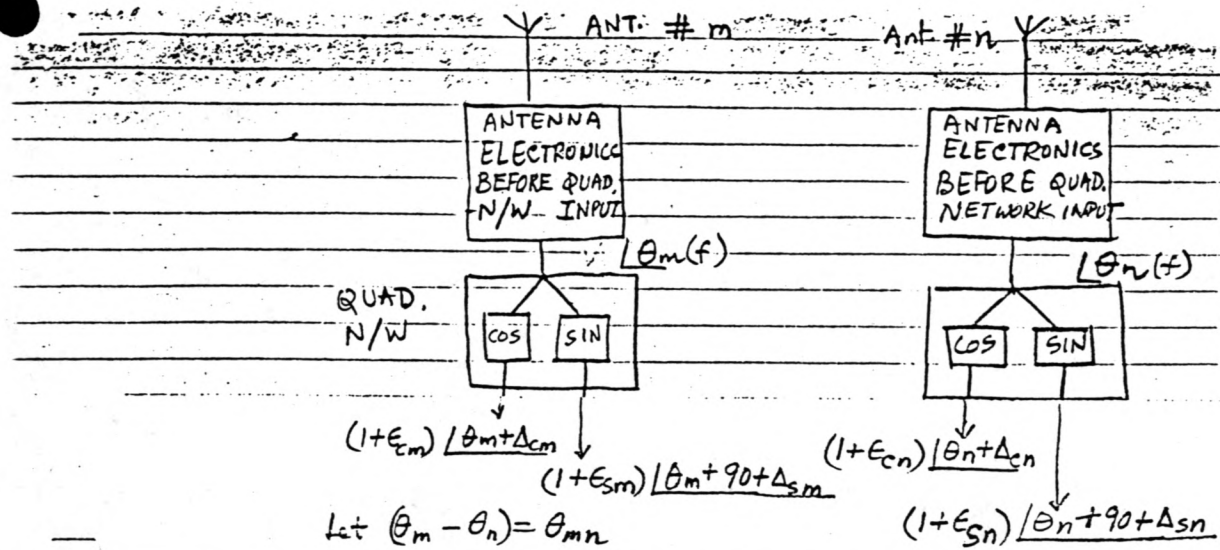
SOURCE NAME:QUA	OBSERV. MODE	BW MHz	DATE	TIME (IAT)		% RMS CLOSURE ERRORS									
				FROM	TO	A Re	Im	B Re	Im	C Re	Im	D Re	Im		
3C84:21	STAND.	CONT	50	86APR15	20:45:50	20:57:30	0.573	0.517	0.538	0.551	0.591	0.502	0.717	0.570	
3C84:22	PH(VA)	CONT	50	86APR15	21:01:00	21:08:00	0.492	0.647	0.544	0.811	0.618	0.538	0.645	0.687	
3C84:23	PH(VX)	CONT	50	86APR15	21:08:20	21:16:00	0.535	0.582	0.538	0.508	0.572	0.543	0.627	0.568	
3C84:31	STAND.	CONT	50	86APR15	23:16:40	23:28:00	0.571	0.535	0.563	0.519	0.588	0.512	0.69	0.585	
3C84:32	PH(VA)	CONT	50	86APR15	23:29:50	23:38:20	0.493	0.68	0.608	0.544	0.598	0.569	0.602	0.627	
3C84:33	PH(VX)	CONT	50	86APR15	23:38:50	23:46:30	0.546	0.617	0.569	0.509	0.552	0.523	0.657	0.596	
3C84:41	STAND.	CONT	50	86APR16	01:54:20	02:06:20	0.595	0.509	0.547	0.536	0.577	0.531	0.669	0.579	
3C84:42	PH(VA)	CONT	50	86APR16	02:06:50	02:16:30	484	0.659	0.558	0.555	0.581	0.565	0.598	0.631	
3C84:43	PH(VX)	CONT	50	86APR16	02:17:00	02:21:20	0.59	0.579	0.553	0.521	0.581	0.551	0.669	0.585	
DIFFERENCES FOR QUALIFIERS						DURATION	APART	% RMS OF DIFFERENCES OF CLOSURE ERRORS							
21-31	STAND	CONT	50	1.5	Hrs.	0.399	0.413	0.302	0.362	0.449	0.423	0.414	0.453		
31-41	STAND	CONT	50	1.5	Hrs.	0.38	0.393	0.296	0.319	0.414	0.371	0.371	0.378		
21-41	STAND	CONT	50	3.0	Hrs.	0.469	0.473	0.329	0.403	0.493		0.396	0.473		
22-32	PH(VA)	CONT	50	1.5	Hrs.	0.255	0.112	0.422	0.619	0.266	0.197	0.246	0.343		
32-42	PH(VA)	CONT	50	1.5	Hrs.	0.222	0.094	0.341	0.129	0.210	0.121	0.216	0.147		
22-42	PH(VA)	CONT	50	3.0	Hrs.	0.262	0.110	0.290	0.632	0.318	0.243	0.273	0.367		
23-33	PH(VX)	CONT	50	1.5	Hrs.	0.365	0.32	0.293	0.274	0.379	0.38	0.331	0.322		
33-43	PH(VX)	CONT	50	1.5	Hrs.	0.389	0.367	0.302	0.307	0.429	0.419	0.378	0.386		
23-43	PH(VX)	CONT	50	3.0	Hrs.	0.43	0.382	0.351	0.33	0.509	0.446	0.457	0.38		



$$\theta_m - \theta_n = \theta_{m,n}$$

Δ 's are errors introduced

Fig. 1 - Block diagram to explain how phasing stabilizes closure-errors.



$$\begin{aligned}
 \text{Re}(m,n)_{\cos \times \cos} &= \langle (1+\epsilon_m) \cos(\theta_m + \Delta_{cm}) \cdot (1+\epsilon_n) \cos(\theta_n + \Delta_{cn}) \rangle \\
 &\approx (1+\epsilon_m + \epsilon_n) \cos(\theta_m - \theta_n + \Delta_{cm} - \Delta_{cn}) \\
 &\approx (1+\epsilon_m + \epsilon_n) \left\{ \left[1 - \frac{(\Delta_{cm} - \Delta_{cn})^2}{2} \right] \cos \theta_{mn} - (\Delta_{cm} - \Delta_{cn}) \sin \theta_{mn} \right\} \\
 \text{(Eq. 1a)} \quad &\approx \left[1 - \frac{(\Delta_{cm} - \Delta_{cn})^2}{2} \right] \cos \theta_{mn} - (\Delta_{cm} - \Delta_{cn}) \sin \theta_{mn} + (\epsilon_m + \epsilon_n) \cos \theta_{mn}
 \end{aligned}$$

$$\begin{aligned}
 \text{also, Re}(m,n)_{\sin \times \sin} &= \langle (1+\epsilon_m) \cos(\theta_m + 90 + \Delta_{sm}) \cdot (1+\epsilon_n) \cos(\theta_n + 90 + \Delta_{sn}) \rangle \\
 &\approx (1+\epsilon_m + \epsilon_n) \cos(\theta_m - \theta_n + \Delta_{sm} - \Delta_{sn}) \\
 \text{(Eq. 2a)} \quad &\approx \left[1 - \frac{(\Delta_{sm} - \Delta_{sn})^2}{2} \right] \cos \theta_{mn} - (\Delta_{sm} - \Delta_{sn}) \sin \theta_{mn} + (\epsilon_m + \epsilon_n) \cos \theta_{mn}
 \end{aligned}$$

$$\begin{aligned}
 \text{Im}(m,n)_{\cos \times \sin} &= \langle (1+\epsilon_m) \cos(\theta_m + \Delta_{cm}) \cdot (1+\epsilon_n) \cos(\theta_n + 90 + \Delta_{sn}) \rangle \\
 &\approx (1+\epsilon_m + \epsilon_n) \cos(\theta_m - \theta_n - 90 + \Delta_{cm} - \Delta_{sn}) \\
 \text{(Eq. 3a)} \quad &\approx \left[1 - \frac{(\Delta_{cm} - \Delta_{sn})^2}{2} \right] \sin \theta_{mn} - (\Delta_{cm} - \Delta_{sn}) \cos \theta_{mn} + (\epsilon_m + \epsilon_n) \sin \theta_{mn}
 \end{aligned}$$

$$\begin{aligned}
 \text{also, Im}(m,n)_{\sin \times \cos} &= \langle (1+\epsilon_m) \cos(\theta_m + 90 + \Delta_{sm}) \cdot (1+\epsilon_n) \cos(\theta_n + \Delta_{cn}) \rangle \\
 &\approx (1+\epsilon_m + \epsilon_n) \cos(\theta_m - \theta_n + 90 + \Delta_{sm} - \Delta_{cn}) \\
 \text{(Eq. 4a)} \quad &\approx - \left\{ \left[1 - \frac{(\Delta_{sm} - \Delta_{cn})^2}{2} \right] \sin \theta_{mn} - (\Delta_{cn} - \Delta_{sm}) \cos \theta_{mn} + (\epsilon_m + \epsilon_n) \sin \theta_{mn} \right\}
 \end{aligned}$$

Fig. 2 Block diagram to explain how phasing stabilizes closure errors when amplitude and phase errors are included

CONTINUUM OBSERVATIONS (USED ONLY A & C IFs) 50MHZ BAND WIDTH,
 AFTER SETTING DELAYS TO ~1ns PHASED ARRAY OBSERVATIONS, BASELINE
 CALIBRATED NATURAL WEIGHING.

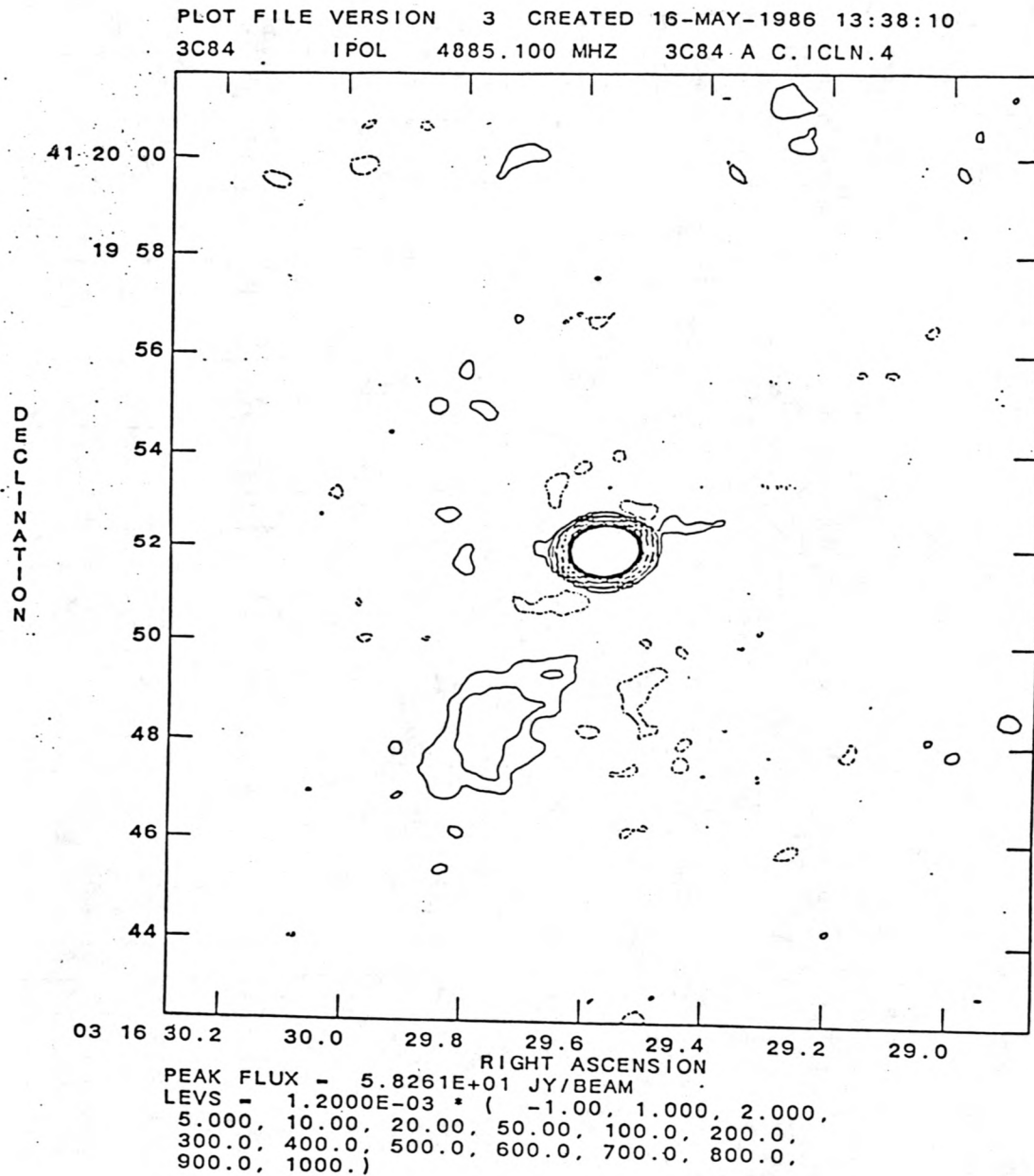


Fig. 3 Continuum observations of 3C84 in A-array configuration of VLA at 6cm with 50MHz bandwidth in phased array mode. Observations were on 86 APR 23 after setting fixed delays to <1nsec accuracy. The map was made with ~3 hours of A & C IF data spread over about 11 hours of time. Data was corrected before making the map assuming constant defects for each baseline and calibrating all visibility points (using BCAL1 and BCAL2 programs available in AIPS).